Microstructure and origin of dislocation etch pits in GaN epilayers grown by metal organic chemical vapor deposition

L. Lu,[1] Z. Y. Gao,[2] B. Shen,[1,a)] F. J. Xu,[1] S. Huang,[1] Z. L. Miao,[1] Y. Hao,[2] Z. J. Yang,[1] G. Y. Zhang,[1] X. P. Zhang,[3] J. Xu,[3] and D. P. Yu[3]
[1]*State Key Laboratory of Artificial Microstructure and Mesoscopic Physics, School of Physics, Peking University, Beijing 100871, China*
[2]*Institute of Microelectronics, Xidian University, Xi'an 710071, China*
[3]*Electron Microscope Laboratory, Peking University, Beijing 100871, China*

(Received 7 September 2008; accepted 31 October 2008; published online 22 December 2008)

Morphology and microstructure of dislocation etch pits in GaN epilayers etched by molten KOH have been investigated by atomic force microscopy, scanning electron microscopy, and transmission electron microscopy (TEM). Three types of etch pits (α, β, and γ) are observed. The α type etch pit shows an inversed trapezoidal shape, the β one has a triangular shape, and the γ type one has a combination of triangular and trapezoidal shapes. TEM observation shows that α, β, and γ types etch pits originate from screw, edge, and mixed-type threading dislocations (TDs), respectively. For the screw-type TD, it is easily etched along the steps that the dislocation terminates, and consequently, a small Ga-polar plane is formed to prevent further vertical etching. For the edge-type TD, it is easily etched along the dislocation line. Since the mixed-type TDs have both screw and edge components, the γ type etch pit has a combination of α and β type shapes. It is also found that the chemical stabilization of Ga-polar surface plays an important role in the formation of various types of dislocation etch pits. © *2008 American Institute of Physics*. [DOI: 10.1063/1.3042230]

I. INTRODUCTION

Wet etching techniques are extensively used for defect evaluation due to its merits of low cost and simple experimental procedure.[1–16] The shapes of etch pits are well correlated with types of defects, and the etch pits density (EPD) may correspond to the density of defects. However, for GaN, the density, types, and distribution of defects vary significantly due to growth-related conditions, which makes it difficult to reach an agreement about the origin of the etch pits, and it can be even more difficult for test techniques.

Generally there are two ways to investigate the relationship between the etch pits and the threading dislocations (TDs) in GaN epilayers, i.e., direct observation and quantitative analysis. Transmission electron microscopy (TEM) works in the first way, while quantitative analysis combines several test technique results such as TEM and x-ray diffraction. It is observed that both the screw-type and mixed-type dislocations terminated at the bottom of etch pits by cross-sectional TEM,[2,3] while it is also found that only nanopipes can cause etch pits by plan-view TEM.[4–6] Visconti *et al.*[7–10] and Xu *et al.*[11] found that the total dislocation density obtained by TEM is close to the EPD, while Kozawa *et al.*[12] found the EPD is smaller than the dislocation density. Besides, the edge-type dislocations related with etch pits cannot be found through direct observation, which was ascribed to the difficulty in preparing a cross-sectional TEM sample.[3] However, the mechanism and origin of dislocations etch pits in GaN epilayer are still ambiguous. In this study, we study dislocation etch pits etched by molten KOH to identify the origin and mechanism of etch pits in GaN epilayer. It is clarified that three types of the etch pits with three shapes originate from screw-, edge-, and mixed-type TDs, respectively. It is also found that the chemical stabilization of Ga-polar surface plays an important role in the formation of various types of dislocation etch pits.

II. EXPERIMENTAL PROCEDURE

GaN epitaxial thin films were grown by means of metal organic chemical vapor deposition on *c*-plane sapphire substrates. Trimethylgallium and NH_3 were used as precursors. High purity H_2 was used as carrier gas. Prior to the GaN growth, the substrate was cleaned under H_2 ambient at 1010 °C. Then, a 20 nm thick low temperature GaN nucleation layer was grown at 560 °C. The annealing stage comprised the ramping stage and the stabilization stage. Then, a 2 μm thick GaN epilayer was grown. Wet etching was performed in molten KOH for 2, 4, 6, and 8 min at 220 and 240 °C, respectively. Surface morphology of samples was characterized by atomic force microscopy (AFM) of Digital Instruments Nanoscope III and scanning electron microscopy (SEM) of Quanta 200FEG. TEM specimens were thinned by conventional mechanical polishing and then Ar-ion milling with 4.5 keV at 5° glancing incidence by Gatan model 691 ion polishing system. Both plan-view and cross-sectional TEM images were performed using JEOL-200CX operated at 160 kV.

III. RESULTS AND DISCUSSION

Figure 1(a) shows a typical SEM image of the GaN surface etched at 220 °C for 4 min. Three kinds of hexagonal etch pits marked by α, β, and γ are observed. Magnified images of three etch pits are shown in Figs. 1(b1), 1(c1), and

a)Electronic mail: bshen@pku.edu.cn.

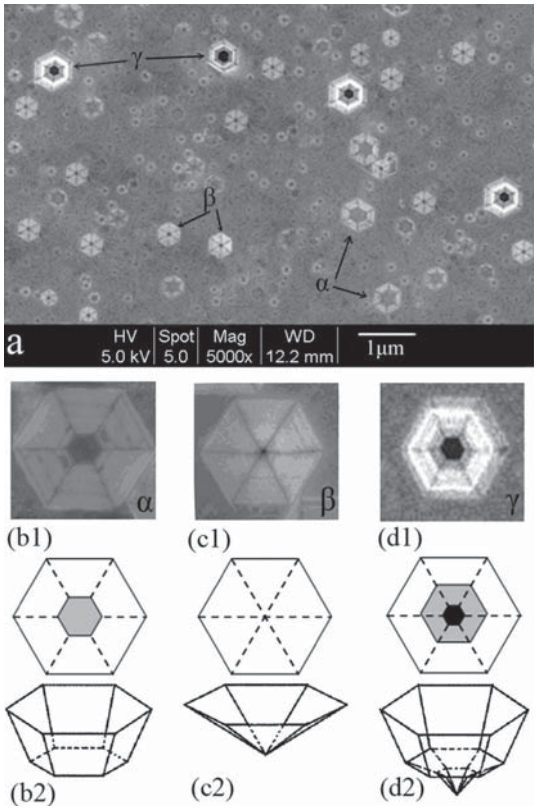

FIG. 1. (a) A typical SEM image of KOH etched GaN surface. (b1) α type, (c1) β type, and (d1) γ type etch pit are observed correspondingly. Two-dimensional and 3D schematic view of (b2) α type, (c2) β type, and (d2) γ type etch pit are demonstrated.

1(d1) respectively. According to the topographic contrast principle of secondary electron image, the brightest part represents a steep incline, the gray area should be a plane or a gentle incline, and the black core means that there is a hole or a sharp groove whose secondary electron cannot be collected. Therefore, schematic shapes of these kinds of etch pits are proposed and shown in Figs. 1(b2), 1(c2), and 1(d2). From Fig. 1(a), it is found that the α type etch pit is an inversed truncated hexagonal pit, the β type one is an inversed hexagonal pyramid, and the γ one is just a polygon but unclear. The following AFM and TEM observations will confirm the proposed illustrations and clarify the shape of the γ type etch pit.

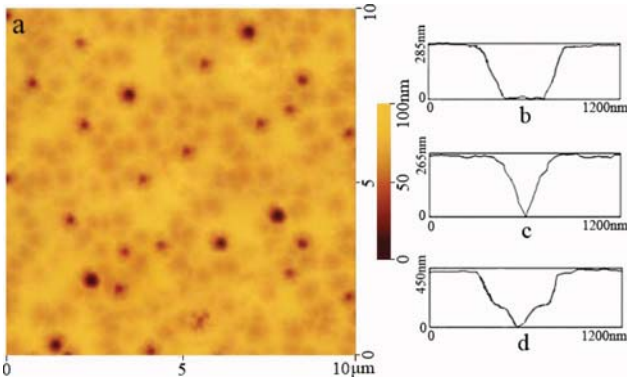

FIG. 2. (Color online) Typical AFM images of KOH etched GaN surface. The etch pits selected to perform line profile in each image are (a) α type, (b) β type, and (c) γ type etch pit, respectively.

Figure 2(a) shows AFM surface image (10×10 μm^2 scan area) of the typical GaN sample. In Figs. 2(b)–2(d), the line profile across the etch pits in symmetry axis is used to show the shape of these etch pits. In Fig. 2(b), the trapezoidal profile is similar to the three-dimensional (3D) schematic illustration shown in Fig. 1(b). In Fig. 2(c), the triangular profile is similar to the 3D schematic view of β type etch pit shown in Fig. 1(c). In Fig. 2(d), the profile of the pit has a triangular and trapezoidal shape. It seems to be a combination of α and β types. The profile in Fig. 2(d) is similar to the 3D schematic view drawn in Fig. 1(d), which is supposed to be the shape of the γ type etch pit.

In principle, TEM can reveal and identify each individual dislocation directly through its strain field. For GaN grown on *c*-plane sapphire, the *c* axis is along [0001]. Therefore we easily obtain zone axis [0001] patterns in a plan-view image and a cross-section image with $\boldsymbol{g}=[11-20]$. Most of the TDs away from the film/sapphire interface have a [0001] line direction. The Burgers vectors for the different types of TDs are $\boldsymbol{a}=1/3\langle11-20\rangle$ (edge-type), $\boldsymbol{c}=\langle0001\rangle$ (screw-type), and $\boldsymbol{c}+\boldsymbol{a}=1/3\langle11-23\rangle$ (mixed-type). As is well known,[17,18] screw-type dislocations are invisible in a TEM image if $\boldsymbol{g}\cdot\boldsymbol{b}=0$ and edge-type dislocations are invisible if both $\boldsymbol{g}\cdot\boldsymbol{b}=0$ and $\boldsymbol{g}\cdot\boldsymbol{b}\times\boldsymbol{u}=0$ ($\boldsymbol{g}$ is the diffractive vector, $\boldsymbol{b}$ is the Burgers vector of the dislocation, and $\boldsymbol{u}$ is the line direction of the dislocation). However, GaN has a hexagonal crystal structure and therefore the basal plane (i.e., 0001) and all planes perpendicular to it are elastic symmetry planes. As a result, all dislocations lying on the basal plane or perpendicular to it exhibit pseudoelastic isotropy and the invisibility criteria for elastically isotropic materials are valid for dislocation, which lie on such planes.[13] In order to study the microstructure of the dislocation etch pits and identify the types of TDs in GaN, many TEM images have been obtained in the same region under weak beam conditions using different $\boldsymbol{g}$ vectors of [0002], [11−20], [01−10], [10−11], and [−2201], respectively. Based on the visibility criteria $\boldsymbol{g}\cdot\boldsymbol{b}=0$, screw and mixed type TDs are observable with $\boldsymbol{g}=[0002]$, while edge and mixed type TDs are observable with $\boldsymbol{g}=[11-20]$. From all images with different $\boldsymbol{g}$ vectors (many images are not shown here), we can identify the types of TDs in GaN.

Figure 3 shows typical cross-sectional TEM images of (a) α, (b) β, and (c) γ types of etch pits, respectively. In Fig. 3(a), the etch pit has a trapezoidal shape. It is consistent with the 3D view of the α type etch pit. A screw-type TD is terminated at the bottom of the pit. So it indicates that α type etch pits correspond with screw-type TDs. A triangular etch pit with an edge-type TD is shown in Fig. 3(b). It is similar to the image shown in Fig. 1(c). Therefore, β type etch pits correspond with edge-type TDs. In Fig. 3(c), the etch pit has a combination of triangular and trapezoidal shapes, and a mixed-type TD is terminated at the sharp bottom of the pit. Here it is confirmed that the given shape of the γ type etch pit is correct, and γ type etch pits correspond with mixed-type TDs.

The density of α, β, and γ type etch pits and the dislocation density obtained by plan view TEM images for typical samples are listed in Table I. The total number of TDs is the

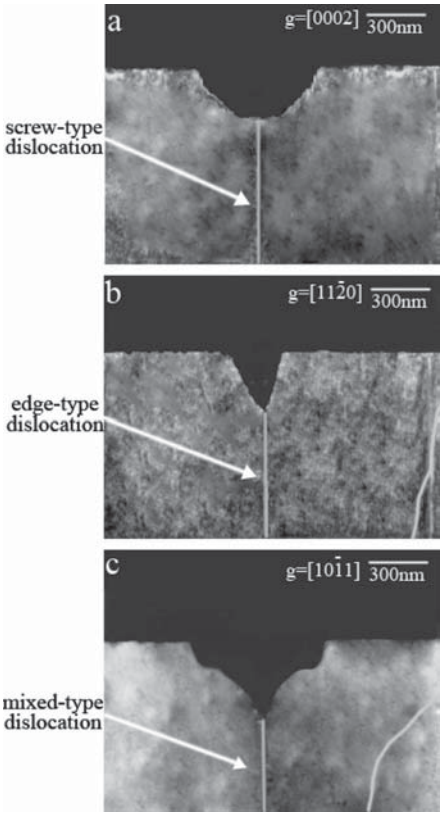

FIG. 3. Cross-sectional TEM images of (a) α type, (b) β type, and (c) γ type etch pit, respectively.

same as consistent with the total of β and γ type etch pits. As discussed previously, β and γ type etch pits should, therefore, correspond with edge-type TDs and mixed-type TDs, respectively.

The above experimental results are consistent with what Hino *et al.*[3] observed. Hino *et al.*[3] found different etch pits correspond to different TDs and concluded that TDs having a screw-component burgers vector act as strong nonradiative centers in GaN epitaxial layers, whereas edge dislocations, which are the majority, do not act as nonradiative centers. However, the mechanism and origin of dislocations etch pits in GaN epilayer are not clarified in their work.

In order to interpret the origin of etch pits, an etching mechanism model confirmed by TEM, SEM, and AFM is proposed. It is believed that α type etch pits represent the surface termination of screw-type TDs. It is well known that

TABLE I. Summary of the etch-pits densities (α, β, and γ type) obtained using the etching technique and the dislocation density determined by means of plan-view TEM for typical samples.

	Etch-pits density			
	α type (cm^{-2})	β type (cm^{-2})	γ type (cm^{-2})	Plan-view TEM dislocation density (cm^{-2})
A	0.98×10^{8}	2.14×10^{9}	1.09×10^{8}	2.19×10^{9}
B	1.12×10^{8}	2.98×10^{9}	1.33×10^{8}	3.11×10^{9}
C	1.53×10^{8}	3.65×10^{9}	1.85×10^{8}	3.62×10^{9}
D	1.49×10^{8}	3.12×10^{9}	1.56×10^{8}	3.08×10^{9}

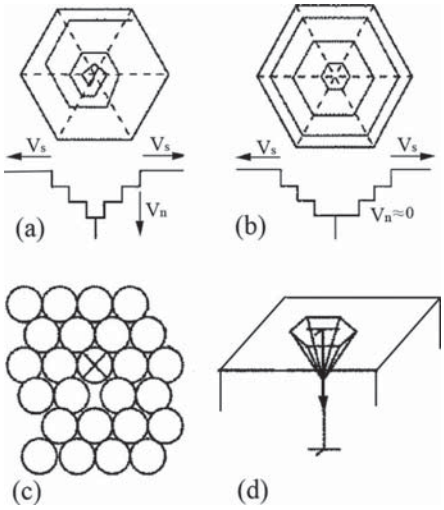

FIG. 4. (a) A few spiral steps formed at the beginning of etching a screw-type TD, (b) the formation of small Ga-face to prevent further vertical etching, (c) an illustration of an edge-type TD, and (d) etching is easier to carry on along the vertical dislocation line.

a screw-type TD creates a step when it terminates at the GaN surface, as shown in Fig. 4(a). This step is associated with the natural terrace structure. At the beginning, etching enlarges the step and forms a few spiral steps, as shown in Fig. 4(a). These spiral steps are so vulnerable that they can be easily attacked by OH^{-1} through further etching. Then only a small plane is left, as shown in Fig. 4(b). This small facet must be Ga-terminated. Even it was N-terminated, it would be further etched to Ga-terminated due to the chemical stabilization of Ga face.[19–23] Once the small smooth plane is formed, the vertical etching velocity (V_n) will become much smaller than the transverse etching velocity (V_s), and finally the small plane will become a bigger one. Therefore, the screw-type TD can be etched to an inversed truncated pyramid.

On the other hand, β type etch pits relate to edge-type TDs. Figure 4(c) illustrates an edge-type TD with $\boldsymbol{b}=\langle 11-20\rangle/3$. "×" denotes the edge-type TD line, which is vertical to the surface. Since every atom in this line has a dangling bond, these atoms are so vulnerable that they can be attacked. There is little chance that a small Ga-terminated facet will form to stop vertical etching as in the case of screw-type TDs. So the edge-type TD can be etched to an inversed pyramid, as shown in Fig. 4(d).

Besides, γ type etch pits are associated with mixed-type TDs. As mixed-type TDs have both screw and edge components, it goes without saying that the shape of γ type etch pits comprises those of α and β type etch pits.

Based on the above analysis, the difference in the etch pits shapes between screw-type TDs and edge-type TDs lies on the etching mechanism model. Etching screw-type TDs depends on the steps created by screw-type TDs, while etching edge-type TDs depends on the dangling bonds along the TDs line. So the emphasis is that the chemical stabilization of Ga-polar surface plays an important part in the formation of dislocation etch pits.

IV. CONCLUSION

Morphology and microstructure of the dislocation etch pits in GaN epilayers etched by molten KOH have been investigated by AFM, SEM, and TEM. Three types of etch pits (α, β, and γ) with different shapes are observed and a model concerning the etching mechanism is proposed to explain their origin. The α type etch pit has an inversed trapezoidal shape, the β one has a triangular shape, and the γ type one has a combination of triangular and trapezoidal shapes. TEM observation shows that α, β, and γ types etch pits correspond with screw, edge, and mixed-type TDs, respectively. For the screw-type TD, it is easily be etched along the steps that the dislocation terminates, and consequently, a small Ga-polar plane is formed to prevent further vertical etching. So the etch pit is an inverted truncated hexagonal pyramid. For the edge-type TD, it is easily etched along the dislocation line, so resulting in an inverted hexagonal pyramid etch pit. Since mixed-type TDs have both screw and edge components, the γ type etch pit has a combination of α and β type shapes. It is also found that the chemical stabilization of Ga-polar surface plays an important role in the formation of various types of dislocation etch pits.

ACKNOWLEDGMENTS

This work is supported by the National Natural Science Foundation of China (Grant Nos. 60325413, 60628402, 10774001, and 60736033), National Basic Research Program of China (Grant Nos. 2006CB604908 and 2006CB921607), the Cultivation Fund of the Key Scientific and Technical Innovation Project, Ministry of Education of China (Project No. 705002), the Research Fund for the Doctoral Program of Higher Education in China (Grant No. 20060001018), and Beijing Natural Science Foundation (Grant No. 4062017).

[1]D. Zhuang and J. H. Edgar, Mater. Sci. Eng., R. **48**, 1 (2005).
[2]K. Shiojima, J. Vac. Sci. Technol. B **18**, 37 (2000).
[3]T. Hino, S. Tomiya, T. Miyajima, and K. Yanashima, Appl. Phys. Lett. **76**, 3421 (2000).
[4]J. L. Weyher, P. D. Brown, J. L. Rouviere, T. Wosinski, and A. R. A. Zauner, J. Cryst. Growth **210**, 151 (2000).
[5]S. K. Hong, B. J. Kim, H. S. Park, Y. Park, and S. Y. Yoon, J. Cryst. Growth **191**, 275 (1998).
[6]S. K. Hong, T. Yao, B. J. Kim, S. Y. Yoon, and T. I. Kim, Appl. Phys. Lett. **77**, 82 (2000).
[7]P. Visconti, K. M. Jones, M. A. Reshchikov, R. Cingolani, H. Morkoc, and R. J. Molnar, Appl. Phys. Lett. **77**, 3532 (2000).
[8]P. Visconti, D. Huang, M. A. Reshchikov, F. Yun, T. King, A. A. Baski, R. Cingolani, C. W. Littion, J. Jasinski, Z. Liliental-Weber, and H. Morkoc¸, Phys. Status Solidi B **228**, 513 (2001).
[9]P. Visconti, D. Huang, F. Yun, M. A. Reshchikov, T. King, R. Cingolani, J. Jasinski, Z. Liliental-Weber, and H. Morkoc, Phys. Status Solidi A **190**, 5 (2002).
[10]P. Visconti, D. Huang, M. A. Reshchikov, F. Yun, R. Cingolani, D. J. Smith, J. Jasinski, W. Swider, Z. Liliental-Weber, and H. Morkoc, Mater. Sci. Eng., B **93**, 229 (2002).
[11]X. Xu, R. P. Vaudo, J. Flynn, and G. R. Brandes, J. Electron. Mater. **31**, 402 (2002).
[12]T. Kozawa, T. Kachi, T. Ohwaki, Y. Taga, N. Koide, and M. Koike, J. Electrochem. Soc. **143**, L17 (1996).
[13]J. Chen, J. F. Wang, H. Wang, J. J. Zhu, S. M. Zhang, D. G. Zhao, D. S. Jiang, and H. Yang, Semicond. Sci. Technol. **21**, 1229 (2006).
[14]C. Youtsey, L. T. Romano, and I. Adesida, Appl. Phys. Lett. **73**, 797 (1998).
[15]J. L. Weyher, F. D. Tichelaar, H. W. Zandbergen, L. Macht, and P. R. Hageman, Appl. Phys. Lett. **90**, 6105 (2001).
[16]M. S. Ferdous, X. Y. Sun, X. Wang, M. N. Fairchild, and S. D. Herseea, J. Appl. Phys. **99**, 096105 (2006).
[17]P. B. Hirsch, A. Howie, R. B. Nicholson, D. W. Pashley, and M. J. Whelan, *Electron Microscopy of Thin Crystals* (Krieger, New York, 1977).
[18]J. F. Nye, *Physical Properties of Crystals* (Oxford University Press, New York, 1975).
[19]D. Huang, P. Visconti, K. M. Jones, M. A. Reshchikov, F. Yun, A. A. Baski, T. King, and H. Morkoc, Appl. Phys. Lett. **78**, 4145 (2001).
[20]T. Palacios, F. Calle, M. Varela, C. Ballesteros, E. Monroy, F. B. Naranjo, M. A. Sanchez-Garcıa, E. Calleja, and E. Munoz, Semicond. Sci. Technol. **15**, 996 (2000).
[21]D. S. Li, M. Sumiya, K. Yoshimura, Y. Suzuki, Y. Fukuda, and S. Fuke, Phys. Status Solidi A **180**, 357 (2000).
[22]D. S. Li, M. Sumiya, S. Fuke, D. Yang, D. Que, Y. Suzuki, and Y. Fukuda, J. Appl. Phys. **90**, 4219 (2001).
[23]B. J. Kim, J. W. Lee, H. S. Park, Y. Park, and T. I. Kim, J. Electron. Mater. **27**, L32 (1998).